A Spintronic Voltage-Controlled Stochastic Oscillator for Event-Driven Random Sampling

H. Lee, C. Grezes, A. Lee, F. Ebrahimi, P. Khalili Amiri, and K. L. Wang, *Fellow, IEEE*

***Abstract*— A voltage-controlled stochastic oscillator (VCSO) utilizing a magnetic tunnel junction (MTJ) is introduced. The VCSO can be used in analog-to-digital information conversion systems for low-energy applications. Experiments show that the thermally activated switching rate of the MTJ is modulated by using an applied voltage across the device via the voltage-controlled magnetic anisotropy effect. The MTJ is deliberately designed to have a relatively short retention time by reducing the perpendicular magnetic anisotropy. The macrospin MTJ compact model is implemented into a circuit design platform as a noise source, which allows the VCSO to generate an event-driven stochastic sampling signal (ESS). Since the average sampling frequency of the ESS is efficiently modulated by the maximum frequency of the input signal, it can drastically reduce the energy consumption of the system. The circuit simulation shows that the frequency range of the ESS and its slope can be optimized by adjusting the MTJ parameters. The VSCO can achieve 20 times improvement in area-efficiency and reduce power consumption by more than three times compared with the previous works.**

***Index Terms*— Magnetic tunnel junction, voltage-controlled stochastic oscillator, perpendicular magnetic anisotropy, voltage controlled magnetic anisotropy, thermal stability, retention time.**

I. Introduction

IN THE era of the Internet of Things (IoT), a tremendous amount of information in the analog domain is sampled and converted to digital data in a large palette of applications such as mobile communications, wearable devices, medical imaging, and radar detection. This digital information is typically processed by a digital signal processor (DSP) or a central/graphics processing unit (CPU/GPU) and stored in memory devices. However, the data deluge significantly increases energy consumption for computations/transmission and requires higher memory capacity to record the data.

One of the promising ways to alleviate these issues is reducing the amount of data by adopting a non-uniform sampling scheme, which is an essential part of compressive sampling (CS) techniques, instead of using a conventional uniform sampling scheme [1]–[3]. Both sampling schemes are briefly described in Fig. 1(a) and (b).

Manuscript received November 22, 2016; revised December 15, 2016; accepted December 17, 2016. Date of publication December 21, 2016; date of current version January 24, 2017. This work was supported by Inston Inc., through a Phase II Small Business Innovation Research Award from the NSF. The review of this letter was arranged by Editor K. J. Kuhn.

The authors are with Inston Inc., Los Angeles, CA 90095 USA, and also with the Department of Electrical Engineering, University of California at Los Angeles, Los Angeles, CA 90095-1594 USA (e-mail: chul0524@ucla.edu).

Color versions of one or more of the figures in this letter are available online at http://ieeexplore.ieee.org.

Digital Object Identifier 10.1109/LED.2016.2642818

The uniform sampling has been developed and optimized in modern hardware and software since the efficient fast Fourier transform (FFT) is executed based on uniformly sampled data. However, using uniform sampling is inefficient in certain types of application, where much of the generated data does not significantly contribute to the overall information. This redundant data increases the computational load, causing energy waste for processing, transmitting and recording of the data [4]. Moreover, uniform sampling cannot efficiently avoid aliasing, leading to distortion in the signal reconstruction [5].

Non-uniform sampling is categorized into two groups: periodic and non-periodic [6]. In the periodic non-uniform sampling, the sampling noise is added to each periodic sampling time; on the other hand, the sampling time of the non-periodic methods is constructed by adding the noise to the previous sampling time, typically called additive random sampling. Another type of non-periodic non-uniform sampling is the level-crossing sampling scheme (LCSS) which takes samples when the input signal crosses predefined threshold levels, referred to event-driven sampling [3]. Non-uniform sampling can have advantages especially with low activity signals such as electrocardiograms and other biological signals, temperature, pressure, voice, and patterns, which remain constant most of the time and change sporadically. Since the total system energy consumption is a function of the sampling rate, event-driven random sampling drastically reduces the computation and data transmission energy by capturing the relevant samples based on the signal characteristic [3]. Also, the randomness of the time interval between samplings improves the dynamic range of the system and addresses aliasing issues [7].

Fig. 1 (c) shows a conventional CMOS-based analog-to-digital information conversion and reconstruction system where the conventional periodic non-uniform clock generator plays a role in determining sampling bandwidth, computational complexity, and overall power consumption. Many periodic non-uniform clock generators have been proposed based on a linear feedback shift register (LFSR) that randomly selects one clock signal among a matrix of ring oscillators, which have different frequencies and phases [8]–[11]. However, these circuits require a large number of transistors and additional controllers, resulting in area and energy consumption overhead, and only provide a fixed average sampling frequency.

We propose an alternative approach to address the area and power issues and to provide flexibility in terms of sampling frequency, based on voltage-controlled magnetic tunnel junctions (MTJs). In principle, a CMOS compatible MTJ is a memory device which has two discrete resistance states switched by an electrical or magnetic bias condition. However, if an MTJ is engineered to have sufficiently low thermal

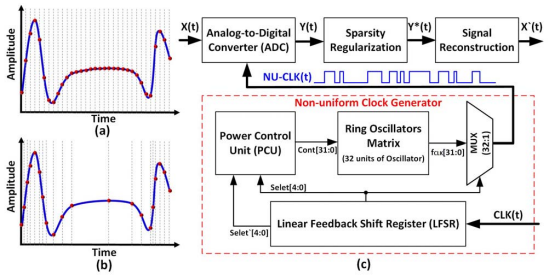

Fig. 1. (a) Uniform sampling that has a constant time interval between samples. (b) Non-uniform sampling which has a variable time interval between samples. (c) Non-uniform clock based analog to digital information conversion and reconstruction system using a conventional periodic non-uniform clock generator.

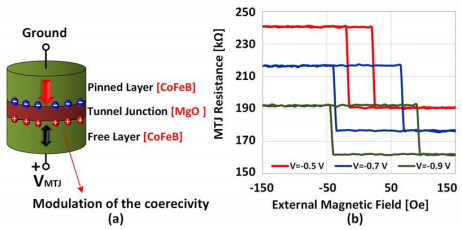

Fig. 2. (a) Voltage dependence of the coercivity. Based on the polarity of the applied voltage, the coercivity of the free layer changes due to the VCMA effect. (b) Measured coercivity with respect to the applied voltage across the device. As the amplitude of the bias increases, the coercivity is enhanced.

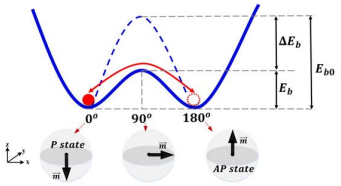

Fig. 3. Schematic of thermally activated switching mechanism. Due to the VCMA effect, the energy barrier E_b can be modulated by the voltage across the MTJ, allowing switching via thermal activation.

stability, the state of the device can be stochastically switched via thermal fluctuations. The average time interval between thermal switching events is called the retention time, which can be modulated by an applied voltage across the MTJ via the VCMA effect. These characteristics allow the MTJ to be used as a voltage-controlled stochastic oscillator (VCSO) that can generate an event-driven stochastic signal (ESS).

The remainder of this letter is organized as follows: Section II briefly explains the physics of the MTJ. Section III introduces the proposed MTJ based VCSO and its simulation results using a macrospin MTJ compact model. The performance of the VCSO is discussed and compared to conventional approaches.

II. Characteristics of Voltage Controlled MTJ

An MTJ consists of two ferromagnetic layers separated by a tunneling barrier as shown in Fig. 2 (a), where the magnetic moment of one layer (free layer) can switch between two directions. Two energetically stable states exist based on the magnetization of the free layer. The parallel state (P) occurs when the magnetic moments of both layers are aligned in the same direction giving rise to a low resistance; while the anti-parallel state (AP) gives rise to a high resistance.

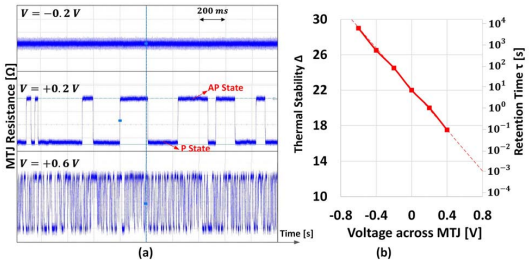

Fig. 4. (a) Measured time domain data of the MTJ's resistance fluctuation under the different electric bias conditions; (b) thermal stability of the measured MTJ with respect to voltage across the device. Retention time is calculated based on the amplitude of the thermal stability at room temperature.

In perpendicularly magnetized MTJs for typical storage memory applications, the interfacial perpendicular magnetic anisotropy (PMA) is enhanced by choosing suitable materials and adjusting the thickness of the ferromagnetic layers (<2 nm) to achieve a high thermal stability ($\Delta > 60$) [12]. In this work, we deliberately engineered the PMA to obtain a relatively low thermal stability (20∼35) for random sampling applications.

In an ultrathin magnetic film structure (e.g. MTJs), an applied voltage across the device can modulate the PMA of the free layer, an effect broadly known as voltage-controlled magnetic anisotropy (VCMA) [13]–[16]. Fig. 2(b) shows the measured corresponding coercivity change of the MTJ (diameter 60 nm, 1.1 nm thick free layer, $\Delta = 22$ at zero bias) as a function of voltages across the device.

The modulation of the coercivity means that the energy barrier $E_b = M_s(H_{k,eff} - \xi \mathrm{V/d})\nu/2$ between the two stable states can be changed by an applied voltage across the MTJ as shown in Fig 3, where $H_{k,eff}$ is the effective magnetic anisotropy, ξ is the VCMA coefficient, ν is the volume of the free layer, d is the tunnel junction thickness, and V is the applied voltage across the MTJ. Since the PMA is a dominant component in the effective magnetic anisotropy ($H_{k,eff}$) of the MTJ, the retention time of the MTJ is modulated by the applied voltage across the device as given by $\tau = \tau_0 \exp(\Delta)$, where τ_0 is equal to 1 ns, thermal stability Δ is equal to $E_b/(k_B T)$, and k_B is the Boltzmann constant. Fig. 4(a) shows measured resistances of the MTJ as a function of time under different bias conditions where a positive voltage decreases the retention time by reducing the thermal stability, while a negative voltage increases the retention time via enhancing the thermal stability, demonstrating the fundamental concept behind this work. The voltage dependence of thermal stability is shown in Fig. 4(b).

III. Proposed Event-Driven VCSO

The macrospin MTJ compact model is implemented into a typical CMOS circuit design platform (e.g. Cadence Virtuoso) [17]. We intentionally adjusted the MTJ model parameters (e.g. $\Delta = 35$ at zero bias, $\xi = 61 \mathrm{fV/mV}$) to allow the MTJ to reliably operate with CMOS supply voltages (1.2 V for 65 nm node) and cover a wider range of frequency. The rationale of using a thermally unstable MTJ in designing a VCSO is as follows: (i) Switching driven by thermal noise is a Poisson process in which the occurrences of certain events

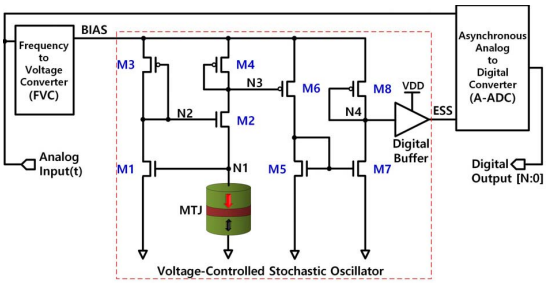

Fig. 5. An MTJ based voltage-controlled stochastic oscillator (VCSO). The switching rate of the MTJ depends on the potential on the BIAS node. The two resistance states of the MTJ are sensed by the amplifier (M6-M7) whose output is converted to an event driven stochastic signal (ESS) via the buffer.

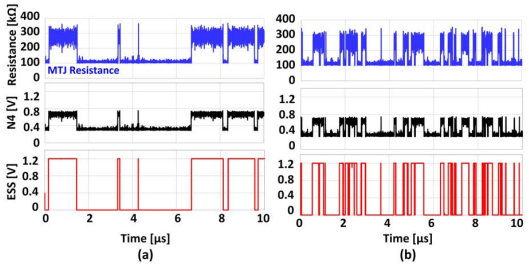

Fig. 6. Transient circuit simulation of the VCSO with the MTJ compact model. The potential on the BIAS node changes the switching rate of the MTJ. The potential of the N1 node is equal to (a) 0.72 V; (b) 0.76 V.

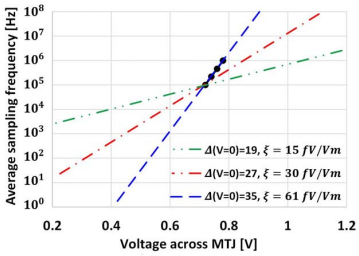

Fig. 7. Average sampling frequency of the VCSO with different thermal stabilities and VCMA coefficients as a function of the voltage across the MTJ.

happen at a certain rate, but completely random, and guarantees non-uniform intervals between samplings; (ii) The voltage dependence of the retention time can be used for realizing event-based sampling; (iii) The two discrete resistance states of the MTJ can be easily converted to a digital signal.

The function of the VCSO in digital information conversion system is as shown in Fig. 5. Based on the frequency of the analog input signal, the VCSO generates an event-driven stochastic signal (ESS) to trigger the asynchronous analog to digital converter (A-ADC) so that the system can efficiently adjust its sampling frequency. The A-ADC samples the analog input signal at each edge of the ESS and converts the input signal into a digitized code based on the signal's amplitude. The average frequency of the ESS is determined by the potential of the BIAS node. The frequency to voltage converter (FVC) converts the maximum frequency of analog input signal into a certain level of voltage on the BIAS node in real time [18], [19]. In the VCSO, the MTJ is connected to the voltage clamp circuit (M1∼M3) and the amplifier (M6∼M8). The voltage clamp maintains the potential on the N1 node regardless of the MTJ resistance fluctuations, which allows the voltage across the MTJ to be purely dependent on the potential of the BIAS node. The circuit operation for generating an ESS is as follows. If the frequency of the input signal is high, the potential of the BIAS node increases, reducing the energy barrier of the MTJ, leading to a higher rate of state switching. If the frequency of the input signal is low, the potential of the BIAS node is low such that the energy barrier of the MTJ remains high, and switching occurs at a slower rate. The MTJ's resistance fluctuation is converted to a voltage variation on the N3 node, which is amplified by the amplifier whose output (N4) is digitized via the buffer, generating the ESS as shown in Fig. 6.

The average sampling frequency of the VCSO exponentially varies as a function of the potential of the BIAS node since the energy barrier decreases linearly as a function of voltage as shown in Fig. 7. The change of switching rate depending on the voltage range across the MTJ can be modulated by engineering the VCMA coefficient. In this simulation, the average sampling frequency can be modulated from 1 kHz to 100 MHz under voltages ranging from 0.6 V to 0.9 V, which indicates that the VCSO can perform wide-dynamic-range random sampling. However, the FVC needs to convert an exponentially varying analog input signal in terms of frequency into a linearized bias voltage via a calibration to reduce errors in the signal reconstruction. Also, to guarantee reliable CMOS operations in the VCSO, the potential on the BIAS node should be larger than 0.6 V so that the amplifier can drive the digital buffer.

TABLE I
PERFORMANCE COMPARISON WITH PREVIOUS WORKS

NUCG	Tech node	Power (μW)	Area (μm^2)
This work	65 nm	< 26.7	10.6
[7]	65 nm	89.7	222.6
[8]	90 nm	115.7	1053.7

The total power consumption of the VCSO is a sum of the power consumption of the analog circuit (M1∼M8) and the digital buffer. The former is mainly proportional to the amplitude of potential on the BIAS node. The latter depends on the switching rate of the MTJ since the dynamic power of the digital buffer is proportional to the number of switching during a certain period.

The number of transistors in designing the VCSO is drastically reduced by taking advantage of the voltage-controlled MTJ. TABLE I summarizes the performance of the VCSO based on the assumption that the average frequency of the ESS is 100MHz.

IV. CONCLUSION

The modulation of the thermally-activated switching rate of the MTJ as a function of voltage has been experimentally observed. Based on this phenomenon, we designed a VCSO which exploits the voltage controllability of the MTJ retention time via the VCMA effect, and generates the wide-dynamic-range random sampling signal. The MTJ compact model parameters are optimized to be operated with CMOS circuits, allowing the VCSO to reduce the area by 20× and the power consumption by more than 3× compared to previous works.

REFERENCES

[1] M. Ben-Romdhane, C. Rebai, A. Ghazel, P. Desgreys, and P. Loumeau, "Pseudorandom clock signal generation for data conversion in a multi-standard receiver," in *Proc. 3rd Int. Conf. Design Technol. Integr. Syst. Nanosc. Era*, 2008, pp. 1–4, doi: 10.1109/DTIS.2008.4540214.

[2] M. Ben-Romdhane, C. Rebai, K. Grati, A. Ghazel, G. Hechmi, P. Desgreys, and P. Loumeau, "Non-uniform sampled signal reconstruction for multistandard WiMAX/WiFi receiver," in *Proc. IEEE Int. Conf. Signal Process. Commun.*, Nov. 2007, pp. 181–184, doi: 10.1109/ICSPC.2007.4728285.

[3] G. Roa, T. Le Pelleter, A. Bonvilain, A. Chagoya, and L. Fesquet, "Designing ultra-low power systems with non-uniform sampling and event-driven logic," in *Proc. 27th Symp. Integr. Circuits Syst. Design (SBCCI)*, 2014, pp. 1–6, doi: 10.1145/2660540.2660973.

[4] T. Beyrouthy, L. Fesquet, and R. Rolland, "Data sampling and processing: Uniform vs. non-uniform schemes," in *Proc. Int. Conf. Event-Based Control, Commun., Signal Process. (EBCCSP)*, 2015, pp. 1–6, doi: 10.1109/EBCCSP.2015.7300665.

[5] P. S. Wyckoff, "Frequency estimator performance analysis with compressive sensing or non-uniform sampling," in *Proc. IEEE Global Conf. Signal Inf. Process. (GlobalSIP)*, Dec. 2014, pp. 674–678, doi: 10.1109/GlobalSIP.2014.7032203.

[6] E. Masry, "Random sampling and reconstruction of spectra," *Inf. Control*, vol. 19, no. 4, pp. 275–288, 1971, doi: 10.1016/S0019-9958(71)90146-X.

[7] M. A. Davenport, J. N. Laska, J. R. Treichler, and R. G. Baraniuk, "The pros and cons of compressive sensing for wideband signal acquisition: Noise folding versus dynamic range," *IEEE Trans. Signal Process.*, vol. 60, no. 9, pp. 4628–4642, Sep. 2012, doi: 10.1109/TSP.2012.2201149.

[8] M. Osama, L. Gaber, and A. Hussein, "Design of high performance pseudorandom clock generator for compressive sampling applications," in *Proc. 33rd Nat. Radio Sci. Conf. (NRSC)*, 2016, pp. 257–265, doi: 10.1109/NRSC.2016.7450836.

[9] R. Z. Bhatti, K. M. Chugg, and J. Draper, "Standard cell based pseudo-random clock generator for statistical random sampling of digital signals," in *Proc. 50th Midwest Symp. Circuits Syst.*, 2007, pp. 1110–1113, doi: 10.1109/MWSCAS.2007.4488752.

[10] D. Bellasi, L. Bettini, T. Burger, Q. Huang, C. Benkeser, and C. Studer, "A 1.9 GS/s 4-bit sub-Nyquist flash ADC for 3.8 GHz compressive spectrum sensing in 28 nm CMOS," in *Proc. IEEE 57th Int. Midwest Symp. Circuits Syst. (MWSCAS)*, Aug. 2014, pp. 101–104, doi: 10.1109/MWSCAS.2014.6908362.

[11] S. Kose, E. Salman, Z. Ignjatovic, and E. G. Friedman, "Pseudo-random clocking to enhance signal integrity," in *Proc. IEEE Int. SOC Conf.*, Sep. 2008, pp. 47–50, doi: 10.1109/SOCC.2008.4641477.

[12] P. K. Amiri, J. G. Alzate, X. Q. Cai, F. Ebrahimi, Q. Hu, K. Wong, C. Grèzes, H. Lee, G. Yu, X. Li, M. Akyol, Q. Shao, J. A. Katine, J. Langer, B. Ocker, and K. L. Wang, "Electric-field-controlled magnetoelectric RAM: Progress, challenges, and scaling," *IEEE Trans. Magn.*, vol. 51, no. 11, Nov. 2015, Art. no. 3401507, doi: 10.1109/TMAG.2015.2443124.

[13] Y. Shiota, T. Nozaki, F. Bonell, S. Murakami, T. Shinjo, and Y. Suzuki, "Induction of coherent magnetization switching in a few atomic layers of FeCo using voltage pulses," *Nature Mater.*, vol. 11, no. 1, pp. 39–43, Jan. 2012, doi: 10.1038/nmat3172.

[14] J. G. Alzate, P. K. Amiri, P. Upadhyaya, S. S. Cherepov, J. Zhu, M. Lewis, R. Dorrance, J. A. Katine, J. Langer, K. Galatsis, D. Markovic, I. Krivorotov, and K. L. Wang, "Voltage-induced switching of nanoscale magnetic tunnel junctions," in *Proc. Int. Electron Devices Meeting*, 2012, pp. 29.5.1–29.5.4, doi: 10.1109/IEDM.2012.6479130.

[15] S. Kanai, M. Yamanouchi, S. Ikeda, Y. Nakatani, F. Matsukura, and H. Ohno, "Electric field-induced magnetization reversal in a perpendicular-anisotropy CoFeB-MgO magnetic tunnel junction," *Appl. Phys. Lett.*, vol. 101, no. 12, p. 122403, Sep. 2012. [Online]. Available: http://dx.doi.org/10.1063/1.4753816.

[16] K. L. Wang, J. G. Alzate, and P. K. Amiri, "Low-power non-volatile spintronic memory: STT-RAM and beyond," *J. Phys. D, Appl. Phys.*, vol. 46, no. 7, p. 74003, Feb. 2013. [Online]. Available: http://dx.doi.org/10.1088/0022-3727/46/7/074003

[17] D. S. Matic, "A magnetic tunnel junction compact model for STT-RAM and MeRAM," M.S. thesis, Dept. Elect. Eng., Univ. California, Los Angeles, Los Angeles, CA, USA, 2013. [Online]. Available: http://kodiak.ee.ucla.edu/cite/pdf/

[18] A. Djemouai, M. Sawan, and M. Slamani, "New circuit techniques based on a high performance frequency-to-voltage converter," in *Proc. 6th IEEE Int. Conf. Electron., Circuits Syst. (ICECS)*, vol. 1. Sep. 1999, pp. 13–16, doi: 10.1109/ICECS.1999.812212.

[19] Y. Gao, K. Abouda, R. Beges, and P. Besse, "Study of frequency-to-voltage converter immunity to fast transient pulses," in *Proc. Asia–Pacific Int. Symp. Electromagn. Compat. (APEMC)*, 2016, pp. 849–851, doi: 10.1109/APEMC.2016.7522887.